



The Geological and Mineralogical Characterization of the Drill Core Samples from the Granitic Gneiss Rock in Wadi Abu Rushied Area, South Eastern Desert, Egypt

Mahmoud, M. A. M.

Nuclear Materials Authority (NMA)

ABSTRACT: The granitic gneiss from a tectono-metamorphic complex exposed along Wadi Abu Rushied area in the Sikait-Abu Rushied district, south Eastern Desert, Egypt, is considered as the key domain of the Arabian-Nubian Shield having very complex structures. The subsurface study of granitic gneiss at Wadi Abu Rushied area has been subjected to geological, mineralogical and radiometric characteristics to constrain the borehole-3(BH3).

Through 32m depth of the studied BH3, the lithology observations reveal the whitish gray granoblastic gneiss (Wg) and presence of sedimentary matrix intersliced with gneiss (Gs) as a sandwiched between two layers of Grayish white granoblastic gneiss (Gg1 and Gg2). The Wg zone is characterized by whitish gray color, fractured and coarse grains with gneissose texture. The Gg1 and Gg2 zone is characterized by dark gray to grayish white color, massive, low fractured contents and have grain size ranged between medium to coarse with gneissose texture. The Gs zone enriched in quartz, biotite and hornblende minerals.

Petrographically, Gneissic rocks (Wg, Gg1 & Gg2) of the studied BH3 consist of quartz, K-feldspars, plagioclase minerals, alternating with biotite, hornblende flakes, muscovite and metasomatic minerals forming gneissose texture, while the metasedimentary matrix enriched in biotite, quartz, hornblende, and feldspars.

There is a dearth of information about the distribution of trace elements in the studied rocks in drilled boreholes at Wadi Abu Rushied area, despite some reports on trace element composition. In the studied BH3, the rocks are enrichment in Zn, Zr, Sr, Y, Rb and Pb, and poor in Ni, Ga and V. Some trace elements are decrease with increasing depth, while the others increase with depth.

The mineralization investigations illustrate that the Uranophane, Thorite and Uranothorite minerals were decreased with the increasing depth, while Zircon, Columbite, Sulphides and other accessories are increase with depth. Radioactive minerals are detected and the highest one is related to the first three meters of the studied borehole.

Radiometrically, the studied BH3 has a moderately to high content of eU and eTh and it has been utilized to identify the uranium migration. Investigation of Wg zone and Gg2 zone shows positive values of uranium migration, indicating that uranium migration is inward the geologic unit. The Gs zone and the Gg1 zone show negative values of uranium migration, indicating that uranium leaching is outward from the geologic unit toward surrounding rock units.

Keywords; drill boreholes, Granoblastic, gneiss, Uranium, migration, pyrite, fractures

I. INTRODUCTION

Abu Rusheid-Sikait district is bordering to the major shear zone named by the Nugrus thrust fault [1], the Nugrus strike-slip fault [2] or Sha'it-Nugrus shear zone [3]. The Nugrus major thrust runs along the upper

part of Wadi Sikait in a NW direction till the southern tip of Gabal Ras Sha'it then swings to a south westward direction along Wadi Sha'it west of Gabel Migif. The Migif-Hafafit gneisses comprise the foot wall of the Nugrus thrust, while the Ghadir group comprises its hanging wall [4].

Wadi Abu Rusheid area is considered as a key domain of the Arabian-Nubian Shield having very complex lithology and structures. It characterizes by low topographic features, and dissects by Khor Abalea, several gullies with two NNW-SSE and ENE-WSW shear zones.

Wadi Abu Rushied area is considered as the south Eastern extension of the Migif-Hafafit metamorphic complex [5]; [6]; [7]; [8], which is highly tectonized and mineralized.

Metamorphic rocks at Abu Rushied area are intruded by intr-acratonic gabbroic and granitic pulses [9]; [10]; [11]; [12]; [13]. These rocks are subjected to polycyclic deformation and metamorphism. It is characterized by regional WNW–ESE thrusting; such thrusting is assigned to an age 682 Ma.y, and between 565 to 600 Ma.y [14].

II. SURFACE GEOLOGY

Details surface studies were carried out on the mineralized zone at Abu Rusheid gneissic rocks, which identified as psammitic gneiss [15]; [16]; [17]; [18]; [19], gneissose granite [20]; [21], cataclastic rocks [22], peralkalic granitic gneisses and cataclastic to mylonitic rocks [23] and highly mylonitic gneissose granitic rock, ranging in composition from granodiorites to adamellites [20].

Wadi Abu Rushied area lies southwest Marsa Alam City in the south Eastern Desert, Egypt. It is bounded by latitudes 24° 36' 43" and 24° 38' 26"N and longitudes 34° 45' 00" and 34° 45' 35"E. It is considered as a multi-mineralized zone for uranium, thorium, economic and other nuclear elements.

Geologic map was constructed to shows the lithology of Wadi Abu Rushied area, which comprises of gneissic rock, ophiolitic mélange and granitic rocks as the main lithologic units (Fig. 1). To explore the uranium mineralization and associated economic minerals at deeper levels, more subsurface data was carried out by Diamond core drilling of many numbers of boreholes.

III. SUBSURFACE STUDY

The boreholes-3 (BH3) was chosen in this paper for the geological and mineralogical study, as well as to illustrate the distribution of uranium (U), thorium (Th) with associating economic minerals at deeper levels. The BH3 has a drilling angle (90°) and depth drilled about 32m., with borehole diameter (76mm.). It is located at the entrance of Khor Abalea in Wadi Abu Rushied area at intersection of latitude, 24° 37' 3.11" and longitude 34° 45' 11.12" (Figs. 1 & 2). The subsurface rocks in the BH3 at Wadi Abu Rushied area characterize the ductile and brittle deformed, intensely mylonitic granitic gneiss.

3.1-Drilling technique

A drilling machine as a crawler mounted "Diamec 262" drilling rig was used, which characterized by diamond core bit, core barrel and water as circulating fluid . The recovered core samples were collected directly from the core barrel of length three meters and arranged in a wooden boxes using "zigzag Arrangement" in which the core samples are arranged from left to right and from right to left. The core samples are labeled with the letter "T" on the top part of each core sample (Fig. 2).

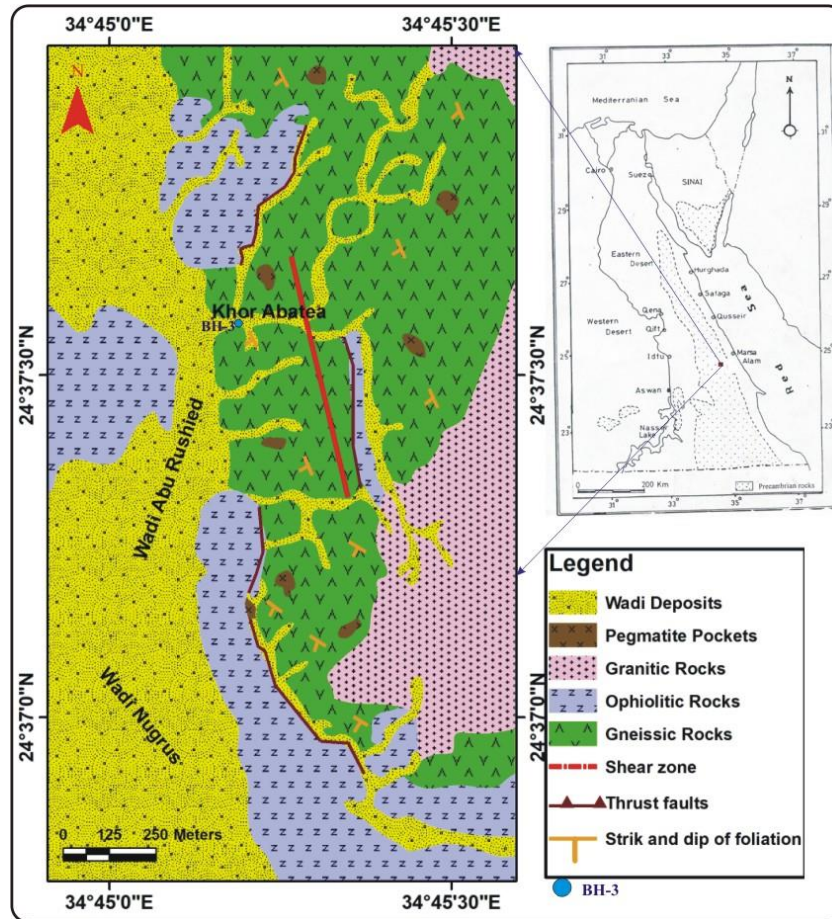


Fig. (1): Geologic map of Wadi Abu Rusheid area showing the lithology and the location of the studied borehole (BH3), South Eastern Desert, Egypt.



Fig. (2): Photographs showing “Diamec 262” drilling rig machine at BH3 in Khor Abalea, Wadi Abu Rusheid area.

3.2-Lithology

The studied handspacmens core samples of BH3 are described from top to bottom (Fig. 3) as; whitish Gray granoblastic gneiss (Wg zone), grayish white granoblastic gneiss (Gg1 zone), metasedimentary matrix intersliced with gneiss (Gs zone) and grayish white granoblastic gneiss (Gg2 zone).

Depth (m.)	Lithology	Degree of deformation	Core recovery	Remarks			
0	Wg	High	88%	- Highly sheared samples. - Enriched by disseminated sulphides. - Visible muscovite increase with depth.			
1							
2							
3		Medium					
4							
5							
6		Low					
7							
8							
9		Gg1			Medium to high	92%	- Medium to highly sheared samples. - Fractures filled with high content sulphides - Quartz veinlets and biotite flakes were found.
10							
11							
12							
13							
14							
15							
16							
17							
18							
19							
20							
21							
22							
23							
24	Gg2	Low	95%	- Fractures filled with sulphides.			
25							
26							
27							
28							
29							
30							
31							
32							

Whitish Gray granoblastic gneiss (Wg)

Gneiss layers intersliced with schist layers (Gs)

Grayish white granoblastic gneiss (Gg)

Fig. (3): Lithologic log of BH3 showing the distribution of different lithological varieties.

3.2.1-Whitish gray granoblastic gneiss (Wg)

The Wg zone is characterized by to whitish gray color, massive, high to medium deformation and having a grain size ranged between medium to coarse grains with gneissose texture (Fig. 4a). It occupies about 21m., of depth from the surface. Secondary uranium minerals as yellow amorphous spots associated with iron oxides filling the late stage fractures at the first three meters of the studied borehole (Fig. 4b). Pyrite is the main Sulphides minerals, which is considered as the source of iron oxy-hydroxides. It is seen as visible grains and disseminated in the studied core samples especially along the fractures, with increasing depth (Fig. 4c).

3.2.2-Grayish white granoblastic gneiss (Gg1 & Gg2)

The Gg1 and Gg2 zones is characterized by to grayish white color, massive, medium to low deformation and having grain size ranged between small to medium grains. It is occupies depth from level 22 to 25m. (Gg1), and repeated again from 30m., until the bottom 32m (Gg2) of the studied borehole. From the depth (30m.) to the depth (32m.), the studied core samples are enriched by altered sulphides due to desulphitization processes of pyrite under oxidizing conditions (Fig. 4d). Shearing and fracturing are dominant (Fig. 4e).

3.2.3-Metasedimentary matrix intersliced with gneiss (Gs)

The Gs zone of the BH3 is present as a sandwiched zone between two zones of grayish white granoblastic gneiss (Fig. 3), with thickness about 4m (from 25.9m. to 29m.). In this zone the studied core

samples are composed of gneiss intersliced with layers of schist (Fig. 4f). The schist rocks are quartz-feldspar-biotite schist, hornblende-biotite-carbonate schist and mica schist [13]; [19]. Quartz-feldspar-biotite schist is characterized by whitish black color, fine to medium grained (Fig. 4g), while hornblende-biotite-carbonate schist is mainly blackish green in color, medium to coarse grained (Fig. 4h).



Fig. (4): Photographs showing the description of core samples in the BH3 at Wadi Abu Rusheid area; A) Well-developed gneissic bands in gneissic rocks., B) Spots of secondary uranium minerals staining on the fracture plane from 1-3m depth in gneissic rocks., C) Sulphides along the fractures plane in gneissic rocks., D) Iron oxides refilled the vugs of dissolved pyrite minerals in gneissic rocks., E) Brecciating along the fractures in gneissic rocks., F) Gneissic layer alternated with layers of mica schist in metasedimentary matrix zone., G) quartz-feldspar-biotite schist in metasedimentary matrix zone., H) hornblende-biotite-carbonate schist in metasedimentary matrix zone.

3.3-Petrography

Ten representative samples of granitic gneisses and metasedimentary matrix were preferably selected for petrographic thin sections, based on observed field relationships between the lithologic units, which include (5) samples from Wg zone, 2 samples from Gg1 zone, 2 samples from Gs zone and 1 sample from Gg2 zone. This study is devoted to the petrographic characteristics of the different lithologic units of the BH3 at Abu Rusheid area. The petrographic characteristics will help in deciphering the petrochemical evolution of the gneisses that may lead to indication of their U-fertility. In this aspect, the petrographic studies were carried out in Nuclear Materials Authority, using a Nikon (Optiphot-pol) polarizing Microscope equipped with a full automatic photomicrographic attachment (modal Microflex AFX-II).

3.3.1-Gneissic rocks

Gneissic rocks (*Wg, Gg1 & Gg2*) of the studied BH3 consist of quartz, K-feldspars, plagioclase minerals, alternating with biotite, hornblende flakes, muscovite and metasomatic minerals forming gneissose texture (Fig. 5a). The metasedimentary matrix (Gs) composed mainly of biotite, quartz, hornblende, and feldspars. The occurrence of hornblende in Abu Rushied granitic gneiss suggests metaluminous character [24]; [25].

Quartz is the most dominant mineral, which possess a remarkable deformation with variable degrees. It is characterized by panidiomorphic to hypidiomorphic crystals with corroded boundaries preserving their wavy extinction (Fig. 5b).

Feldspars are formed as K-feldspar and plagioclase minerals, which K-feldspars are mainly represented by orthoclase, perthite and microcline (Fig. 5c), occurring as xenomorphic crystals, while plagioclase appears as xenomorphic crystals with uniform direction in albitic twinning (Fig. 5E).

Brown, reddish brown to greenish brown biotite flakes occur as a small to medium size with a distinctive pleochroic scheme, and it is alternating with the quartzo feldspathic components to produce the gneissose texture (Fig. 5a). Biotite is stretched parallel to its longest axis, and partially altered to chlorite.

Zircon, uranothorite, and monazite are accessory minerals, where zoned zircon reflects tetragonal crystals habits with short/long prismatic forms. Due to intensively tectonized such as sheared and fractured boundaries, some of radioactivity minerals are found leading to metamictized phenomenon in zircon (Figs. 5d & e). Sometimes, pleochroic halos are found when zircon is impeded in biotite flakes. Well-formed tetragonal crystals of Uranothorite occur in brown color, coated by iron oxides and surrounded by radial veinlets of quartz grains (Fig. 5f). Opaque minerals are mantled by yellow amorphous materials, which they characterized the radioactive minerals (Fig. 5g).

3.3.2-Metasedimentary matrix (Gs)

Microscopically, the metasedimentary rocks are classified according to the dominant minerals into; quartz feldspar biotite schist (quartzo-feldspathic schist), Muscovite schist, and hornblende-biotite-carbonate schist. Quartz feldspar biotite schist composes of quartz, plagioclase, perthite and biotite, while Opaque, zircon and allanite are accessories. Quartz feldspar biotite schist is characterized by schistose structure where quartz and feldspars are highly deformed. The hornblende-biotite-carbonate schist characterized by schistose structure and mainly composed of quartz, biotite, hornblende and some carbonate minerals with lesser amount of altered fine grained feldspar minerals (Fig. 5h).

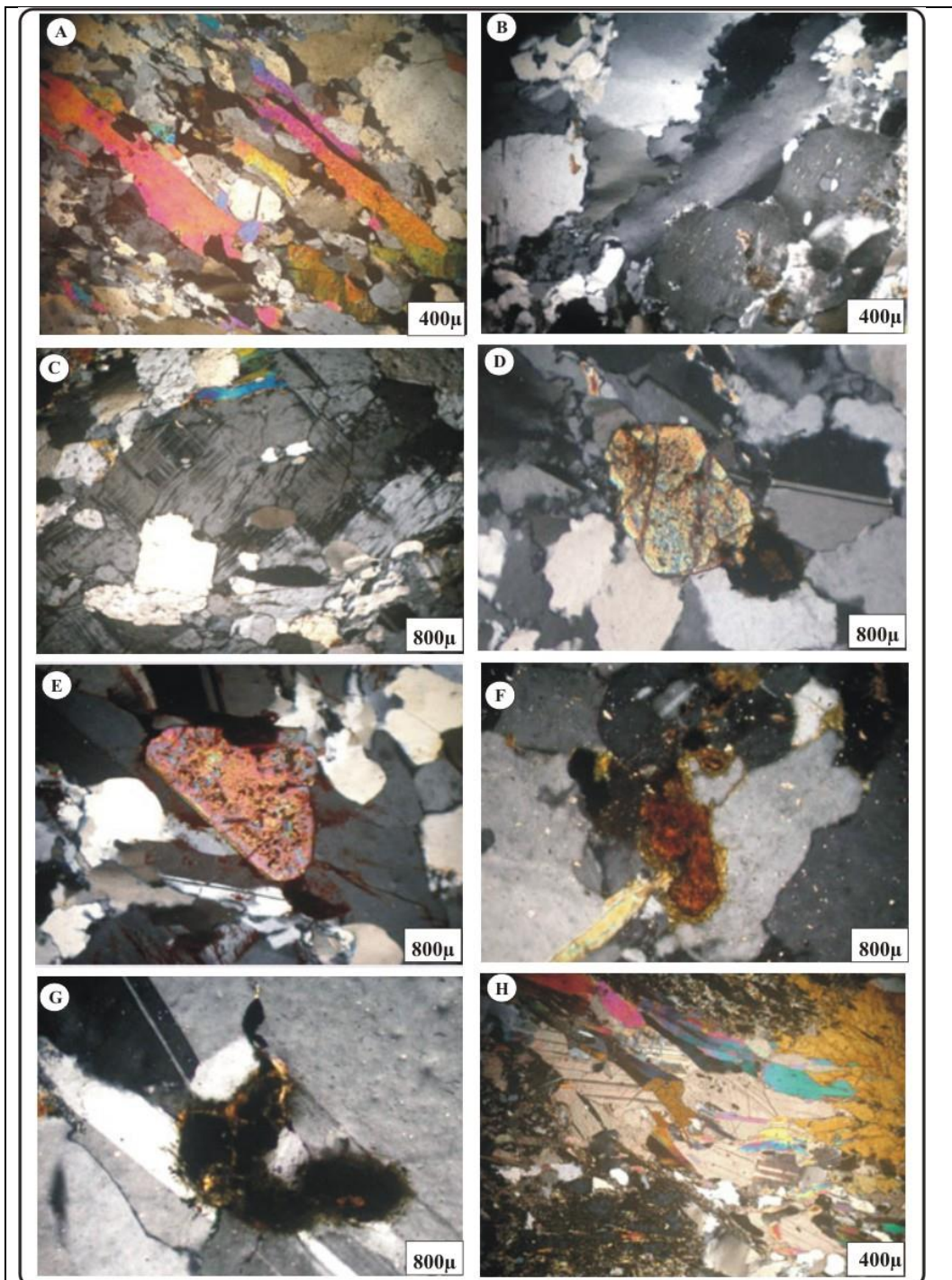


Fig. (5): Microphotographs showing some petrographical characteristics of gneissic rocks and metasedimentary matrix in BH3; A) Stretched crystals of quartz, K-feldspars and plagioclase alternating with biotite forming gneissose texture in gneissic rocks., B) Oriented crystals of quartz with sutured boundaries associating with pulverized crystal of string perthite in gneissic rocks., C) K-feldspars represented by microcline perthite., D) Fractured and highly sheared zircon crystal in gneissic rocks., E) Zoned and metamict zircon with prefer fracture in gneissic rocks., F) Well-formed tetragonal crystal of uranothorite mineral (U-Th) in gneissic rocks, G) Opaque mineral surrounded by amorphous radioactive material imbedded in plagioclase in gneissic rocks., H) Elongated crystals of calcite, hornblende and biotite forming schistose structure in metasedimentary matrix.

3.4-Trace elements distribution

The geochemical analyses are used to display the chemical signatures of the studied rocks of BH3 at Abu Rushied area. Thirteen (13) chosen samples were then subjected to chemical analysis using wet chemical technique of Shapiro and Brannock (1962) for major oxides and X-ray fluorescence technique (XRF) for trace elements. The obtained data of some trace elements are listed in table (1) and figure (6), which illustrated the following;

Table (1): Trace elements analysis for the BH3, at Abu Rushied area, south Eastern Desert

Depth	Trace elements													Rock units
	Cr	Cu	Ni	Zn	Zr	Ga	Sr	Y	Rb	V	Nb	Pb	Ba	
1-3m	25	21	2	792	1577	7	2329	142	945	2	81	2.3	65	(Wg) zone
4-6m	28	29	2	1094	1637	9	2301	145	1018	2	81	176	73	
7-9m	29	17	3	694	1558	38	2300	140	360	2	79	166	67	
10-12m	30	16	5	509	1650	39	2406	141	1015	2	84	159	63	
13-15m	20	33	4	1360	2301	47	3237	214	1225	3	114	48	64	
16-18m	18	74	5	2143	1820	13	2587	107	607	3	91	67	82	
19-21m	20	71	5	1749	412	22	607	71	632	3	20	40	68	
Aver.	24.3	37	3.7	1192	1565	25	2252	137	829	2.4	78.6	94	68.9	
22-23m	22	107	4	2293	292	37	444	68	407	3	15	38	86	(Gg1) zone
24-25m	21	95	4	2067	1464	4	2085	122	526	5	72	76	160	
Aver.	21.5	101	4	2180	878	21	1265	95	467	4	43.5	57	123	
26-27m	20	84	5	1993	1022	33	1466	105	617	15	51	62	498	(Gs) zone
28-29m	30	125	15	1529	689	6	990	112	213	10	33	96	335	
Aver.	25	105	10	2761	856	19	1228	109	415	13	42	79	417	
30-31m	19	57	5	463	188	16	303	106	429	7	9	85	288	(Gg2) zone
At 32m	15	45	4	399	180	10	300	104	389	7	9	79	254	
Aver.	17	51	4.5	431	184	13	302	105	409	7	9	82	271	

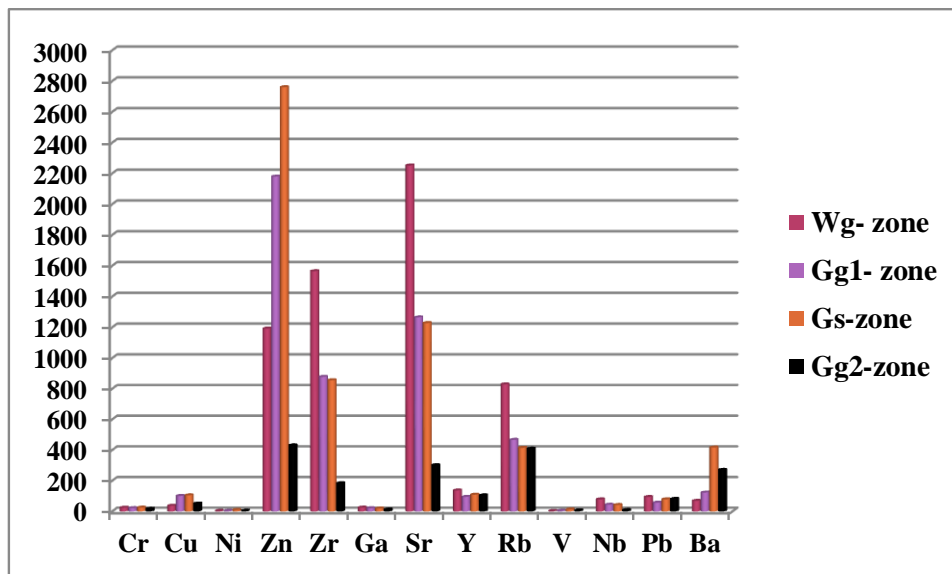


Fig. (6): Histogram showing the distribution of some analyzed trace elements in different lithologic units of BH3, at Abu Rushied area.

-The studied gneissic rocks (Wg, Gg1 and Gg2 zone) of BH3 have low average contents of compatible elements such as vanadium (V), Chromium (Cr), Gallium (Ga) & Nickel (Ni), while they have low to moderate contents in Gs zone. Cr-mineralization is a function of the original pressure, temperature, sulphur and oxygen conditions at

time of formation of the ultramafic rocks. When the studied gneissic rocks, which intruded or lie adjacent to mafic-ultramafic rocks, as in the upper part of BH3, then these gneissic rocks will possess a high *Cr* content.

-The lithophile and high field strength elements (*HFSE*) such as Rubidium (*Rb*), Barium (*Ba*), strontium (*Sr*), Zircon (*Zr*), Yttrium (*Y*) & Niobium (*Nb*) are recorded minerals in the studied area. *Rb*, *Sr*, *Ba* and *Zr* are high contents in *Wg* zone, *Gg1* zone and *Gs* zone, while they are low to moderate in *Gg2* zone.

-Zirconium and Hafnium Hydrolysis of both Zr^{41} and Hf^{41} cations, which mainly reside in zircon, occurs in strongly acidic solutions according to: $M^{41} + 11H_2O_3 \rightarrow MOH_3 + 11H^+$ [26]. Zircon (*Zr*) contents decrease steadily during differentiation, indicating that zircon was present throughout crystallization. This is in compatible with expected low solubility of zircon in low-temperature peraluminous melt [27].

-*Ba*, *Sr* and *Rb* concentrations seemed to be controlled by crystal fractionation, where *Rb* and *Sr* decrease with depth, while *Ba* increases in residual fluids, upon increasing crystallization.

- The *Sr* tends to increase relative to calcium (*Ca*) during fractionation, hence *Ca/Sr* decreases during magmatic crystallization. High plagioclase content in studied rocks caused abnormal increase in the *Sr* content and hence low *Ca/Sr* ratio [28].

-Yttrium (*Y*) reflects moderately to high distribution through the depth of BH3 and it seemed to be highly concentrations in *Wg* zone and *Gs* zone.

-The chalcophile elements such as copper (*Cu*), Zinc (*Zn*) and Lead (*Pb*) are abundant in the studied core samples of BH3. *Cu* and *Pb* possess low to moderately average contents in the studied rocks, while *Zn* possess highly content in *Wg* zone, *G1* zone and *Gs* zone and low to moderately content in *Gg2* zone.

-Niobium (Nb^{51}) has the similar geochemical behavior with Tantalum (Ta^{51}), and titanium (Ti^{41}), due to the close similarities in ionic radii: (0.64, 0.68, 0.61Å, respectively). In many rock-forming titanium minerals (e.g., titanite) a certain proportion of *Ti* is replaced by *Nb* or *Ta* [29]; [30].

-Gallium and aluminum display similar characteristics in natural systems, where the ionic radii of both cations are so similar that most of the gallium is present in *Al* minerals, mainly feldspars. If any diversity is observed in the behavior of *Ga* and *Al* during weathering or alteration, it may be due to the higher solubility of gallium compounds in weakly alkaline or neutral solutions [31].

3.5-Mineralization

The studied core samples of the BH3 were firstly disaggregated by crushing using a small hummer and sieved using the size fraction of 0.5 to +1mm. The chosen samples were subjected to systematic mineral separation procedures to liberate the considered radioactive minerals from the other gangue minerals.

For each sample the size fractions which ranging between 150µm to 600µm were subjected to the heavy liquid separation using Bromoform solution (sp.g. 2.81g/cm³). The heavy fractions were then magnetically fractionated according to their magnetic susceptibilities using Frantz isodynamic separator model L-1 at different current intensities (0.2, 0.5, 1.0 and 1.5 Amp). Mineral grains were picked under binocular microscope depending on the grain shape, color, hardness, and crystal habit.

Some of the separated grains were examined by Environmental Scanning Electron Microscope (ESEM) Phillips EXL130 and attached by EDX unite system. On the other hand, some thin section of studied core samples were also prepared and analyzed by the ESEM. All the former processes were carried out on the laboratories of the Nuclear Materials Authority (NMA), Cairo, Egypt. The mineralization investigations of the studied core samples of BH3 are illustrated and summarized in table (2).

Uranophane

Uranophane is the alteration product of uraninite and appears to be of supergene origin where they can be noticed in the oxidized parts of deposits [32]. There is a positive correlation between the degree of hematization and the intensity of uranium mineralization along altered zone [33]; [34]. This may be due to the ability of iron oxides to adsorb uranium from circulating solutions or due to the prevalence of oxidation conditions that causes the precipitation of uranium as U^{+6} (Uranophane).

In the studied rocks of BH3, the Uranophane grains characterized by massive, radiated and tufted yellow to brownish yellow aggregates as well as dense microcrystalline masses (Fig. 7A).

Sulphides

The base metals in the studied rocks of BH3 are represented by sulfides, especially pyrite. Pyrite (FeS_2) is widely oxidized, thus imparting some parts of the outcrops a reddish color. Pyrite is found as euhedral to subhedral crystals characterized by pale brass yellow color.

Columbite

Columbite is isomorphous minerals belongs to columbite-tantalite series. When niobium predominates, it is called columbite. Tantalite and columbite grade is into one another, where Nb/Ta ratios equal to 11.5 [35]. The U-bearing columbite is Ta-poor (4.9 %) and the U-content (15.8) increases with the decreasing the temperature of crystallization [36]. Columbite is occurred in the studied rocks as black, flattened, prismatic and euhedral to subhedral crystals (Fig. 7B).

Uranothorite

Uranothorite has anhedral, metamict/non metamict crystals (Fig. 7C), sometimes associated with black mica where cleavage does not appear in metamict crystals. Uranothorite is recorded in the studied rocks especially in Wg zone, and decrease with increasing depth.

Zircon

Zircon is a common mineral in igneous rocks and metamorphic rocks particularly in the Na-rich plutonic rocks. It is associated with biotite and quartz. If zircon enclosed by biotite or other colored silicates, it sometimes gives pleochroic haloes due to its content of radioactive elements [37]; [38]; [39].

Rounding shape of zircon can take place in igneous rocks by magmatic adsorption while corrosion shape may be due to metasomatism [29]. The development of bi-pyramidal variety of zircon to crystallization, appaicity of the magma and substitution by U, Th and REEs lead to formation the metamict zircon [40]. Zircon is recorded in all depth of the studied BH3, and it characterized by prismatic and bi-pyramid crystals and has varying of honey colors due to the effect of radioactivity (Fig. 7D).

Cassiterite

Cassiterite is a tin oxide mineral, it is generally opaque, but it is translucent in thin crystals. It is formed in high temperature quartz veins and pegmatite associated with granitic intrusives. Luster and multiple crystal faces produce a desirable gem. Cassiterite is characterized by Pyramidic, prismatic, radially crystals (Fig. 7E), it is concentrated in Gg1 and Gs zone of the studied BH3.

Garnet

Garnet is formed in some granitic pegmatites and in manganese-rich metamorphic rocks. Garnet (spessartine type) is a characteristic mineral in K and Na-metasomatic processes. The formation of spessartine in rocks is considered as an indication for alumina excess in the magma (peraluminous- metaluminous nature) and characteristics for the replacement zones of complex pegmatites containing Li minerals [41]. In the studied rocks, garnet is sub-angular to sub-rounded grains with dark orange color, vitreous luster and white streak (Fig.7f).

Fluorite

Violet fluorite is accessory mineral in the studied rocks of BH3, occurring either as disseminated subhedral grains or as veinlets, which reflects its secondary origin. Fluorite exhibits colorless to pale violet associated with iron oxides (Fig. 7G).

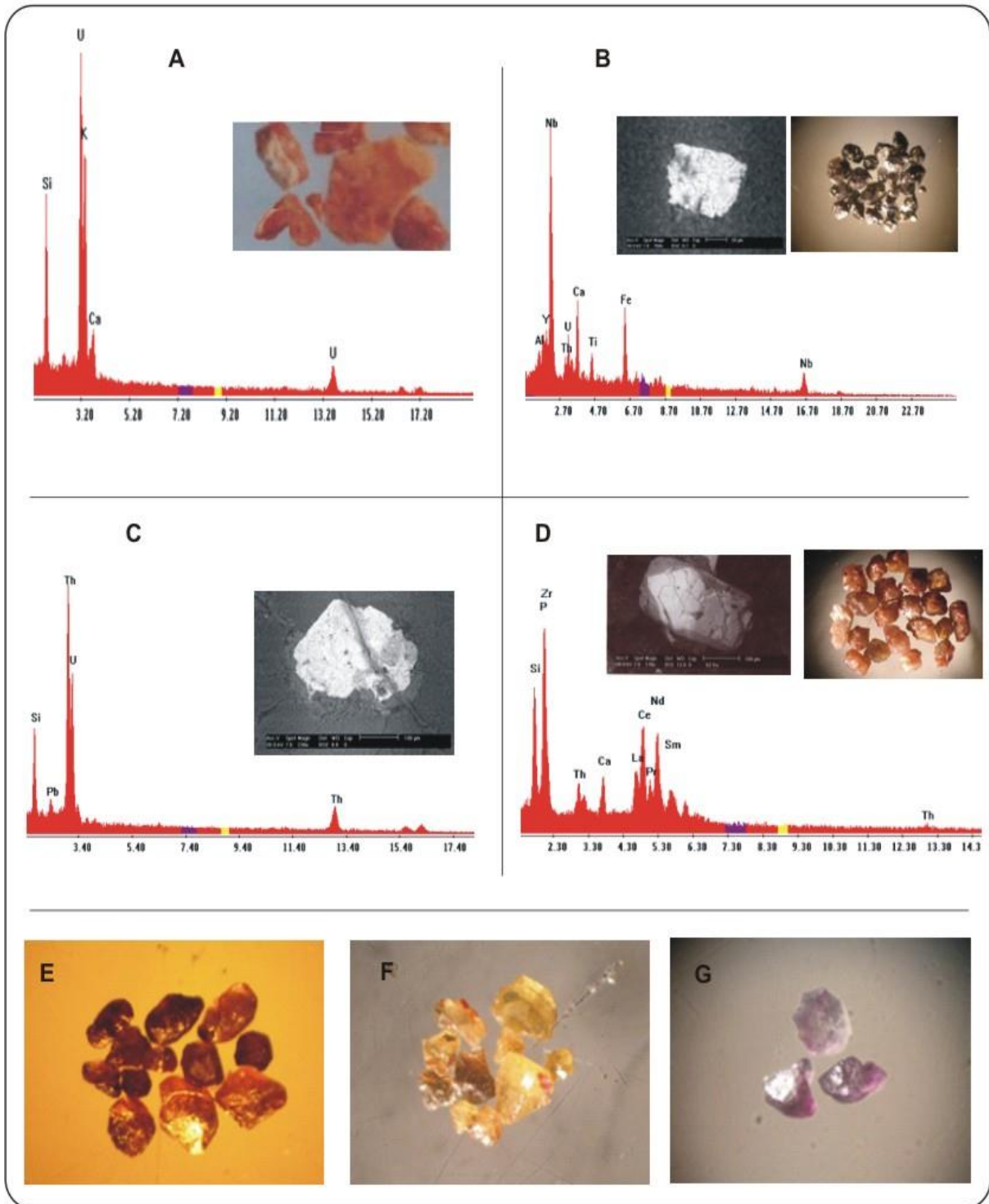


Fig. (7): Photographs, EDX and BSE image for some important minerals in the studied BH3 showing; A) Uranophane grains, b) Columbite grain, C) Uranothorite grains, D) Zircon grains, E) Separated garnet grains, F) Separated cassiterite grains, and G) Separated fluorite grains.

Table (2): Summarized the minerals association in different rock units at the BH3, Wadi Abu Rushied area

Depth	Lithology	Mineral associations
1-3m	Wg zone	Uranophane, Sulphides, Zircon Columbite, Uranothorite, and Garnet
4-6m		
7-9m		
10-12m		
13-15m		
16-18m		
19-21m		
22-23m	Gg1 zone	Zircon, Cassiterite, Sulphides, Garnet, and Columbite
24-25m		
26-27m	Gs zone	Garnet and Uranophane
28-29m		
30-32m	Gg2 zone	Uranothorite, Zircon, Fluorite Sulphides, and Cassiterite,

3.6-Radiometry

Thirteen (13) chosen samples were determined radiometrically for equivalent uranium (eU ppm) and equivalent thorium (eTh ppm) contents by using multi-channel analyzer Gamma-ray detector (Gamma-spectrometer technique). The studied core samples are crushed to about 100 mesh then the containers is filled with about 300-400gm of the crushed samples, sealed well and left for at least 21 days to accumulate free radon for attaining radioactive equilibrium.

The Radiometric measurements were carried out on the studied core samples from the drilled BH3 and the results were measured then related to the standards for U, Th provided by International Atomic Energy Agency (IAEA) and UNSCEAR, (42) and they are listed in table (3).

Table (3): listed eU, eTh, U_m for (13) core samples of the BH3, at Abu Rushied area.

Depth	eU (ppm)	eTh (ppm)	eU/eTh	eTh/eU	Remarks	
1-3m	115	130	0.88	1.13	$U_p = 65.5$ $U_o = 63.8$ $U_m = 1.7$	Wg zone
4-6m	90	115	0.78	1.28		
7-9m	82	105	0.78	1.28		
10-12m	59	75	0.79	1.27		
13-15m	44	55	0.80	1.38		
16-18m	35	48	0.73	1.37		
19-21m	33	59	0.56	1.79		
Aver.	65.4	83.9	0.76	1.36		
22-23m	58	36	1.61	0.62	$U_p = 64$ $U_o = 64.3$ $U_m = -0.3$	Gg1 zone
24-25m	70	35	2.0	0.50		
Aver.	64	35.5	1.81	0.56		
26-27m	19	12	1.58	0.63	$U_p = 19.5$ $U_o = 20.3$ $U_m = -0.8$	Gs zone
28-29m	20	18	1.11	0.90		
Aver.	19.5	15	1.35	0.77		
30-31m	12	23	0.52	1.92	$U_p = 17$ $U_o = 16.7$ $U_m = 0.3$	Gg2 zone
At32	22	30	0.73	1.36		
Aver.	17	26.5	0.63	1.64		

3.6.1-General characteristics

-The uranium content (eU) of Wg zone ranged from 33 to 115ppm., with an average 60.7ppm., and the thorium content (eTh) ranged from 48 to 130ppm., with an average 73.1ppm. The eU/eTh ratio is ranged from 0.50 to 0.88, with an average 0.76, while the eTh/eU ratio ranged from 1.13 to 1.79 with an average 1.36 (Table 3).

-The uranium content (eU) of Gg1 zone ranged from 58 to 70ppm., with an average 64ppm., and the thorium content (eTh) ranged from 35 to 36ppm., with an average 35.5ppm. The eU/eTh ratio is ranged from 1.61 to 2.0, with an average 1.81, while the eTh/eU ratio ranged from 0.50 to 0.62 with an average 0.56 (Table 3).

-The uranium content (eU) of Gs zone ranged from 19 to 20 ppm., with an average 19.5ppm., and the thorium content (eTh) ranged from 12 to 18ppm with an average 15ppm. The eU/eTh ratio is ranged from 1.11 to 1.56, with an average 1.35, while the eTh/eU ratio ranged from 0.63 to 0.90 with an average 0.77 (Table 3).

-The uranium content (eU) of Gg2 zone ranged from 12 to 22 ppm., with an average 17ppm., and the thorium content (eTh) ranged from 23 to 30ppm., with an average 26.5ppm. The eU/eTh ratio is ranged from 0.52 to 0.73, with an average 0.63, while the eTh/eU ratio ranged from 1.36 to 1.92 with an average 1.64 (Table 3).

From table (3) and figure (8), the distribution and variation of eU, eTh, eU/eTh and eTh/eU ratio with depth at the BH3 illustrated that;

-The average values of the eU & eTh contents of the the different rock units are higher than the Clarke values (Clarke value for eU = 4 ppm and for eTh = 18-20 ppm) [43].

-More than one radioactive mineral are detected and the highest one is related to the first three meters of the studied borehole, as well as the eU and eTh values decrease with increasing the depth.

-If the eU content is more than the eTh content, this is regarding to the presence of U-bearing minerals, which are observed in thin section and mineralogical examination.

-If the eTh content is more than the eU content, this is regarding to the presence of Th-bearing minerals, which are observed in thin section and mineralogical examination.

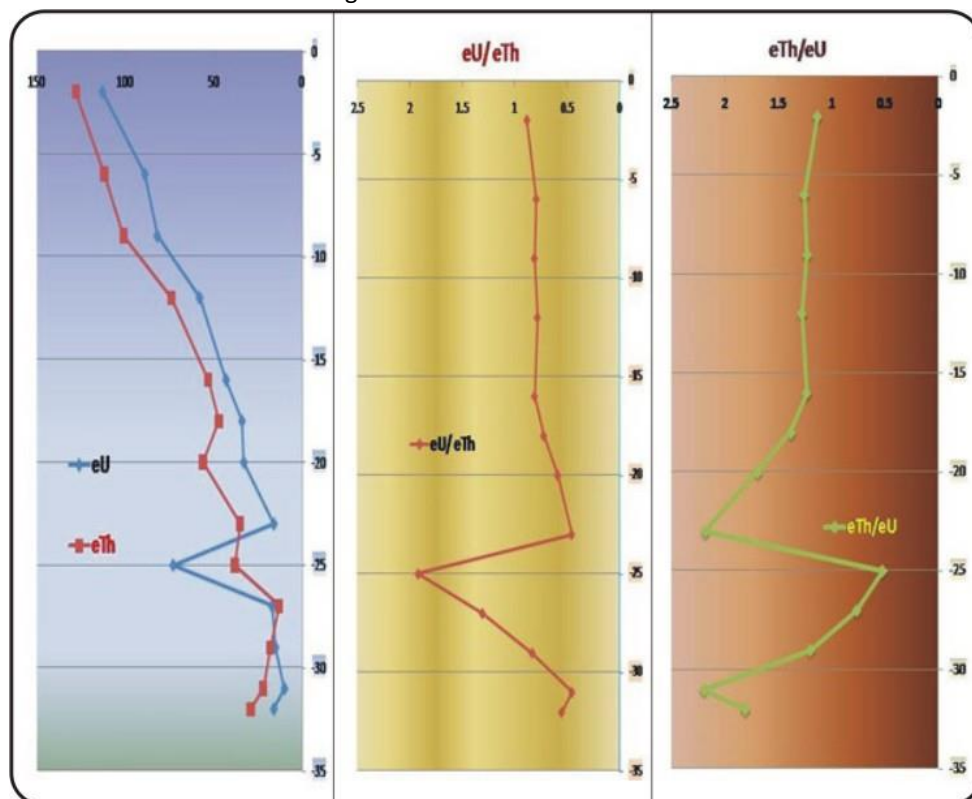


Fig. (8): eU, eTh (ppm), (eTh/eU) and (eU/eTh) ratio with depth of in the studied BH3 at Wadi Abu Rusheid area.

3.6.2-Uranium migration

The accompaniment of Uranium and thorium together in the geologic rocks are due to the similarity in their ionic radii. U^{+4} is easily oxidized and migrates during crustal evolution, while Th is stable in the oxidation zones. Therefore, Th is considered as a reference and can be used, in order to study the state of the original uranium [44]. The half-life periods of U and Th are very long, therefore the actual ratio of eU/eTh can be considered as the original eU/eTh ratio. The eU/eTh ratio being approximately constant in the same geologic unit in a relatively closed environment, therefore it is a very important indicator for uranium migration (out or in) [45]; [46]; [47].

According to the NMA, Internal Scientific Report [48], the uranium migration value (U_m) can be obtained (Table 3) by subtracting the original uranium content (U_0) from the present measured uranium content U_p , as shown in the following equations;

$U_0 = eTh \cdot (eU/eTh) \dots \dots \dots (1)$, where, eTh is the average eTh content (in ppm) and eU/eTh is the average regional eU/eTh ratio for different geologic units.

$U_m = U_p - U_0 \dots \dots \dots (2)$, where, U_p is the average uranium content.

If $U_m > 0$, it reflects that uranium migration is inward the geologic unit, while if $U_m < 0$, it reflects that, uranium migration is outward of the geologic unit.

Based on a careful examination of the statistical results of application of the uranium migration (Table 3), the studied rocks of BH3 reflect the following;

There is the positive values of uranium migration ($U_m = 1.7$) in Wg zone, the negative value of uranium migration ($U_m = -0.3$) in Gg1 zone, the negative value of uranium migration ($U_m = -0.8$) in Gs zone, and the positive values of uranium migration ($U_m = 0.3$) in Gg2 zone.

IV. CONCLUSION

The BH3 is located at the entrance of Khor Abalea in Wadi Abu Rushied area at intersection of latitude, $24^\circ 37' 3.11''$ and longitude $34^\circ 45' 11.12''$. The subsurface rocks are characterized by the ductile and brittle deformation and intensely mylonitic granitic gneiss.

-Whitish Gray granoblastic gneiss (Wg zone), grayish white granoblastic gneiss (Gg1 zone), metasedimentary matrix intersliced with gneiss (Gs zone) and grayish white granoblastic gneiss (Gg2 zone) are described as lithologic units through the BH3.

Gneissic rocks (Wg, Gg1 & Gg2) consist of quartz, K-feldspars, plagioclase minerals, alternating with biotite, hornblende flakes, muscovite and metasomatic minerals forming gneissose texture.

The studied rocks of the BH3 are chiefly higher in lithophile trace elements, while they are as well as moderately in chalcophile elements, believed that the original substances forming these granites are from earth's crust due to contamination.

The Uranophane, Thorite and Uranothorite minerals were decreased with the increasing depth. Zircon, Columbite, Sulphides and other accessories are increase with increasing depth.

The radioactive minerals (especially Uranophane) were noticed at the first three meters of the BH3 as secondary uranium minerals along the fractures. These minerals appear as yellow spots on the surface of the samples.

There is the positive values of uranium migration ($U_m = 1.7$) in Wg zone, the negative value of uranium migration ($U_m = -0.3$) in Gg1 zone, the negative value of uranium migration ($U_m = -0.8$) in Gs zone, and the positive values of uranium migration ($U_m = 0.3$) in Gg2 zone. If $U_m > 0$, it reflects that uranium migration is inward the geologic unit, while if $U_m < 0$, it reflects that, uranium migration is outward of the geologic unit.

V. REFERENCE

1. Greiling, R. O., Kröner, A., El-Ramly, M. F. and Rashwan, A. A., (1988): Structural relations between the southern and central parts of the Eastern Desert of Egypt: details of an fold and thrusts belt. In: El-Gaby, S., Greiling, R. (Eds.), the Pan-African Belt of the NE Africa and Adjacent Areas. Tectonic Evolution and Economic Aspects. Freidr. Vieweg & Sohn, Braunschweig/Weisbaden, 121-145.

2. **Fritz, H., Wallbrecher, E., Khudeir, A. A., Abu El-Ela, F. F. and Dallmeyer, D. R., (1996):** Formation of Neoproterozoic metamorphic core complexes during oblique convergence Eastern Desert, Egypt. *J. African Earth Sci.*, 23,311–329.from the Bauda Desert, Sudan., *J. Afr. Earth Sci.*, vol. 3, p. 61-75.
3. **Fowler, A. and Osman, A. F. (2009):** The Shait-Nugrus shear zone separating central and south Eastern Deserts, Egypt: A post-arc collision low-angle normal ductile shear zone, *Journal of African Earth Sciences*, 53: 16-32.
4. **El-Bayoumi, R. M. A., (1984):** Ophiolites and mélange complex of Wadi Ghadir, Eastern Desert, Egypt. *Bull. Fac. Earth Sci.*, King Abdul-Aziz Univ., Jeddah, 6, 324-329.
5. **El-Ramly, M. F. and Akaad, M. K., (1960):** The basement complex in the central E. D., Egypt. Between lat. 24° 30' and 25° 40' N. *geol. Surv., Egypt*, pp. 8- 35.
6. **Hassan, M. A. (1964):** Geology and petrographical studies of the radioactive minerals and rocks in Wadi Sikait Wadi El Gemal area. Eastern Desert, U. A. R: M. Sc. Thesis faculty of science, Cairo Univ. 165p.
7. **El-Shazly, E. M. and Hassan, M. A. (1972):** Geology and radioactive mineralization at Wadi Sikait-Wadi El Gemal area. South EasternDesert, Egypt. *J.Geol. V.2*, 201p.
8. **Hashad, A. H. and Hassan, M. A. (1959):** Report on the prospection work carried out in Wadi El Gemal area, south Eastern Desert, Egypt. Internal Report, AEE, Cairo, UAR.
9. **Saleh, G. M. (1997):** The potentiality of uranium occurrences in Wadi Nugrus area, southeastern Desert, Egypt. Ph. D. Thesis Mans. Univ. 171p.
10. **Assaf, H.S., Ibrahim, M.E., Zalata, A.A., El- Metwally, A.A. and Saleh, G.M. (2000):** Polyphase folding in Nugrus-Sikait area south Eastern Desert, Egypt. *JKAW: Earth Sci.*, 12, 1-16 p.
11. **Ibrahim, M. E. Saleh, G. M., Mahmoud, F. O., Abu El Hassan, E. A., Ibrahim, I. H. Aly, M. A., Azab, M. S., Rashed. M. A., Khaleal, F. M. and Mohamed, A. M., (2004):** Uranium and associated rare metals potentialities of Abu Rusheid brecciated shear zone, south Eastern Desert, Egypt. (Internal Report) Part II.
12. **Khaleal, F. M. (2005):** Geologic evaluation of some rare metal resources in Nugrus–Sikait area, Eastern Desert, Egypt. Ph.D. thesis, faculty of Science, Al-Azhar University, Egypt, 187pp.
13. **Mahmoud, M. A. M. (2009):** Highlight on the geology, geochemistry and spectrometry of the muscovite granites at Wadi El Gemal area, South Eastern Desert, Egypt, Ph.D. thesis, Faculty of Science Suez Canal University,Egypt,259 PP.
14. **Stern, R. J. and Hedge, C. E. (1985):** Geochronological and isotopic constraints on late Precambrian crustal evolution in the Eastern Desert of Egypt. *Am. J. Sci.*, V. 285, 97-127 p.
15. **Hassan, M. A., 1973:** Geology and geochemistry of radioactive columbite-bearing psammitic gneiss of Wadi Abu Rusheid, South Eastern Desert, Egypt: *Ann. Geol. Surv. Egypt*, v.3, pp. 206-225.
16. **Abd El-Monem, A. A. and Hurley, P. M. (1979):** U-Pb dating of zircon from psammitic gneisses, Wadi Abu Rusheid-Wadi Sikait area, Egypt. In *Evolution and Mineralization of the Arabian–Nubian Shield*.
17. **Hilmy, M.E.; Bayoumi, R. M. and Eid, A. S. (1990):** Geochemistry and mineralization of the psammitic gneiss of the Wadi Abu Rushied, Eastern Desert, Egypt. *J. Afri. Earth Sci.*, 11, 197.
18. **Abd El-Naby, H., and Frisch, W., (2006):** Geochemical constraints from the Hafafit Metamorphic Complex (HMC): Evidence of Neoproterozoic back-arc basin development in the central Eastern Desert of Egypt. *Journal of African Earth Science*, 45, 173-186.
19. **Shalan, A. S. (2016):** Subsurface geological and geochemical studies with uranium distribution for some boreholes in Abu-Rusheid uranium occurrence, southern Eastern Desert, Egypt, Ph.D. thesis, faculty of Science, Al-Azhar university, Egypt,186pp.
20. **Ibrahim, M. E., Assaf, H. S. and Saleh G. M., (2000):** Geochemical alteration and spectrometric analyses in Abu Rusheid altered uraniferous gneissose granites, South Eastern Desert, Egypt *Chem. Erde* 60, 173-188.
21. **Raslan, M. F., (2008):** Occurrence of Iskikawaite (Uranium-Rich Samarskite) in the mineralized Abu Rushied Gneiss, Southeastern Desert, Egypt. *International Geology Review*. Vol. 50, pp.1132-1140.
22. **Ibrahim, M. E.; Saleh, G. M.; El-Tokhi, M. M. and Rashed. M. (2007a):** A Lamprophyre bearing-REEs in Abu Rusheid area, Southeastern Desert, Egypt. *The 7th Inter. Confer. Geo.*, Alex. Uni., pp.30.
23. **Ali, M. A.; Lentz, D. R. and Hall, D. C. (2011):** Mineralogy and geochemistry of Nb-, Ta-, Sn-, U-, Th-, and Zr-bearing granitic rocks from Abu Rusheid shear zones, South Eastern Desert, Egypt. *Chinese J. Geo-chem.*, 30(2): 226.
24. **Chappell BW, White AJR, (1974):** Two contrasting granite types.*Pac Geol* 8:173-174.

25. **Chappell BW, White AJR (2001):** two contrasting granite types: 25 years later. *Aust J Earth Sci* 48: 489–499.
26. **Baes C.F. and Mesmer R.E. (1976):** *The Hydrolysis of Cations*. John Wiley & Sons.
27. **Waston, E. B., and Harrison, T. M., (1983):** Zircon saturation revisited: Temperature and composition effects in variety of crustal magma type. *Earth Planet. Sci. Lett.* 64, 295-304.
28. **Taylor, S. R., (1965):** The application of trace element data to problems in petrology. In: *Physical and chemistry of the earth* (ed); Ahrens, L.H., Pres. F., Runcor, S.K. and Urey, H.C.P. 133-213.
29. **Deer, W. A., Howie, R. A. and Zussman, J., (1992):** *An introduction to the Rock-Forming minerals*. 2nd Edition, Longman Sci, London. p.696.
30. **Berry, L. G., Mason, B. and Dietrich R. V. (2000):** *Mineralogy*. CBS Publishers and Distributors, New Delhi, India. 561 PP.
31. **Goldschmidt V. M. (1954):** *Geochemistry*. Oxford Press.
32. **Gorman, D. H., and Naffield, E. W., (1955):** Studies of radioactive compound: Uranophane and Beta-uranophane., *An, Min, V* 40, pp 634-645.
33. **FrondeL, J.W. and Fleissner, (1955):** Glossary of uranium and thorium bearing minerals. *U.S. Geol. Survey Bull.* 1015-B. *Geol.*, vol. 83, pp 249-281.
34. **Boyle, R. W. (1982):** Geochemical prospecting for thorium and uranium deposits. *Develop. Economic, Geol.*, 16, El Sevier, Amsterdam, p.489.
35. **Tischendorf, G., (1977):** Geochemical and petrographic characteristics of silicic magmatic rocks associated with rare-metal mineralization. In: *Stemprok, M., Burnol, L. and Tischendorf, G. (Eds.), Metallization associated with acid magmatism, V. 2. Usterdni Ustav Geologicky, Prague. P.* 41-98.
36. **Heinrich, E. W. (1962):** *Mineralogy and geology of radioactive raw materials*. Mc Graw-Hill Book Company, New York.
37. **Zussman, J., Deer, W. A. and Howie, R. A., (1966):** *An introduction to rock forming minerals*, Longmans, London, 517 p.
38. **Speer, J.A. (1982a):** Zircon. In: *Reviews in Mineralogy* (vol. 5: 2nd edition) *Orthosilicates*, Ribbe, P.H. (ed.), pp.67.
39. **Speer, J. A. (1982b):** The actinides orthosilicates. In: *Reviews in Mineralogy* (vol. 5: 2nd edition) *Orthosilicates*, Ribbe, P.H. (ed.), pp. 113.
40. **Pupin, J.P.; Bonin, B.; Tessier, M. and Turco, G. (1978):** Role de l'eau sur les caracteres morphologiques et la cristallisation du zircon dans les granitoides. *Bull. Soc. Géol. Fr.*, S7-XX (5): 721.
41. **Baldwin, J. R., and Van Knorring, O. (1983):** Compositional range of Mn-garnet in zoned granitic pegmatites. *Canda. Mineral.*, 21, 683-688.
42. **UNSCEAR, (2010):** "United Nations Scientific Committee on the Effect of Atomic Radiation, "Sources and Effects of Ionizing Radiation. Radioactivity", 100, 49-53.
43. **Clarke, SPJ., Peterman, ZE., Heier, KS., (1966):** "Abundances in uranium, thorium and potassium. In: *Handbook of physical constants*", vol 97. Geological Society of America Memoirs, New York, pp 521–541.
44. **Aswathanarayana, U. (1985):** In *Principles of Nuclear Geology*. Oxonian Press Pvt. Ltd., New Delhi.
45. **Khalil, A.F., Nigm, A.A., Shata, A.E., Youssef, M.A.S., (2015):** Interpretation of uranium remobilization using ground spectrometric data in North Ras Millan area, Southern Sinai, Egypt. *Egy. J. Appl. Geophys.* 14 (1), 15–31.
46. **Asfahani, J., Aissa, M., Al-Hent, R. (2007):** Uranium migration in sedimentological phosphatic environment in Northern Palmyrides, Al-Awabed Area, Syria. *Appl. Rad. Isot.* 65, 1078–1086.
47. **Asfahani, J., Aissa, M., Al-Hent, R. (2010):** Aerial spectrometric survey for localization of favorable structures for uranium occurrences in Al-Awabed area and its surrounding (Area-3), Northern Palmyrides –Syria. *Appl. Rad. Isot* 68, 219–228.
48. **NMA, (1999):** **A report of work progression during II sub-stages (December, 1998–February, 1999):** on uranium evaluation in Abu-Zeneima Area, Sinai, Egypt. Confidential Report, NMA, Cairo, Egypt.